ISSN: 2993-6594

Research Article

Open Access Journal of Disease and Global Health

Radiotherapy-Induced ECM Remodeling: Implications for Cellular Migration and Tumor Growth from Evidence-Based Modeling

Hasan Jalaeikhoo[1], Hamed Bagheri[1,2,3*], Jalal Kargar[4] and Reza Laripour[5]

[1]*AJA Cancer Research Center (ACRC), AJA University of Medical Sciences, Tehran, Iran*

[2]*Radiation Sciences Research Center (RSRC) AJA University of Medical Sciences, Tehran, Iran*

[3]*Radiation Biology Research Center, Iran University of Medical Sciences,Tehran, Iran*

[4]*School of Medicine AJA University of Medical Sciences, Tehran, Iran*

[5]*Faculty of Medicine, AJA University of Medical Sciences, Tehran, Iran*

[*]Corresponding Author
Hamed Bagheri, AJA Cancer Research Center (ACRC), AJA University of Medical Sciences, Tehran, Iran.

Submitted: 2026, Feb 10; **Accepted:** 2026, Mar 13; **Published:** 2026, Mar 30

Citation: Jalaeikhoo, H., Bagheri, H., Kargar, J., Laripour, R. (2026). Radiotherapy-Induced ECM Remodeling: Implications for Cellular Migration and Tumor Growth from Evidence-Based Modeling. *Ope Acce Jou Dis Glo Heal, 4*(1), 01-10.

Abstract

Cancer progression is governed not only by the intrinsic properties of tumour cells but also by the microenvironment through which they migrate and grow. Here we develop a hierarchical modelling framework to investigate how extracellular matrix (ECM) structure and radiotherapy together shape cell trafficking and tumour evolution. In the first part of this work we model migration in confined environments by representing a single cell as a random walker on a percolation lattice, where occupied bonds mimic ECM fibres and obstacles represent steric barriers. We then extend the model to include radiation-induced remodelling of these fibres, enabling us to quantify how dynamic changes in ECM density and orientation influence motility. In the final stage we couple the percolation-based motility to a simple tumour growth module and implement a cytotoxic effect of radiotherapy on tumour cells. Using this multi-scale model we compare treatment schedules that vary in inter-fraction time and dosage. Our results indicate that intermediate regimens—either shorter inter-fraction intervals or lower per-fraction doses—can reduce tumour burden more effectively than extreme protocols by balancing cytotoxicity with the pro-migratory side effects of ECM remodelling. These findings underscore the importance of jointly considering matrix dynamics and radiation timing when designing radiotherapy schedules.

1. Introduction

Radiotherapy is one of the most widely used modalities for cancer treatment, aiming to destroy tumour cells by inducing DNA damage. While effective in killing cancer cells, growing evidence suggests that radiation also causes long-lasting changes to the tumour microenvironment (TME), particularly the extracellular matrix (ECM), which can inadvertently facilitate tumour recurrence and metastasis [1-3]. The ECM is not merely a structural scaffold; it actively regulates cell behaviour, including adhesion, migration and differentiation [4,5]. Radiation-induced remodelling of the ECM can alter its stiffness and microarchitecture (for example by changing collagen fibre diameter and pore size) and may promote cross-linking, thereby influencing how residual cancer cells interact with their environment [1-3]. More importantly, these alterations might induce new dynamics that allow for further expansion of tumour cells. Despite such indications, side effects of radiotherapy at the tumour level and possible adverse effects are less studied both in silico and in vitro. Such explorations would expand our understanding of lasting effects of radiotherapy and would further incentivise development of more optimised treatments.

ECM stands as a physical barrier against tumour invasion, and many tumours acquire mutations that allow them to alter or degrade the ECM in order to invade nearby tissues [6-8]. ECM structure is such a substantial player that the orientation of its fibrils alone is able to affect cell migration direction [9-13]. Aligned ECM fibrils facilitate mesodermal cell migration towards the animal pole [14]. Alignment of the fibrillar matrix in vitro can control migration, consistent with a role for ECM orientation in promoting the directional migration of these cells in vivo [15,16]. Studies of in vivo explants to analyse breast-cancer metastasis reveal that metastatic tumour cells and macrophages migrate rapidly along collagen fibres [17]. Highly metastatic tumour cells migrate preferentially along fibres. The reticular orientation of the collagen matrix that surrounds the mammary glands may anchor and/or restrain cells [18]. Parallel collagen fibres that radiate outwards from tumour explants can promote tumour epithelial cell invasion, whereas a non-linear matrix reduces invasive behavior [19]. This raises the question of how changes in ECM structure may support cell migration and further growth of tumours.

Mathematical modeling provides a powerful framework to dissect the complex interplay between tumor cells, the extracellular matrix, and therapeutic interventions. Unlike purely experimental approaches, models allow systematic exploration of hypotheses and prediction of outcomes under conditions that may be difficult or impractical to test in the laboratory. In cancer research, modeling has been widely used to capture processes such as tumor growth dynamics, angiogenesis, cell migration, and treatment response [20-22]. In the context of radiotherapy, mathematical models have helped to elucidate dose–response relationships, optimize fractionation schedules, and investigate the microenvironmental consequences of treatment [23,24]. Importantly, lattice-based and percolation-style models have proven effective in capturing how spatial heterogeneity of tissue structure influences cancer invasion and therapy outcomes [25,26]. By bridging biological mechanisms with quantitative abstraction, mathematical models provide essential insight into the competing forces of cytotoxicity and pro-migratory microenvironmental remodeling, thereby guiding the development of more effective therapeutic strategies.

The goal of this paper is to build a sequence of increasingly detailed models to dissect these coupled phenomena. We begin by formulating a minimal percolation-based model for single-cell migration in a static ECM. This framework captures how heterogeneous fibre networks and steric obstacles govern migration in confined environments. Inspired by experimental reports of radiation-induced ECM remodelling, we next incorporate dynamic bond renewal to represent fibre turnover and realignment. We quantify how this remodelling alters transport properties and identify parameter regimes that optimise cell displacement. Finally, we extend the model to include tumour growth dynamics and the direct cytotoxic effects of radiotherapy on cells. This extension allows us to evaluate different treatment schedules by coupling motility with population dynamics. Using the final model we show that intermediate regimens—either shorter intervals between radiation pulses or lower per-fraction doses—can minimise adverse microenvironmental side effects while maintaining tumour control.

2. Model

To investigate ECM remodelling we model the microenvironment as a dynamic bond–percolation lattice. Each bond (edge) is present with probability p and absent with probability $1-p$, representing ECM fibres and pores respectively. We introduce three characteristic time scales: the hopping time τ_{hop}, the renewal time τ_{ren} and the observation time τ_{obs}. The hopping time denotes the mean interval between two successive attempts of a cell to move to a neighbouring lattice site. The renewal time sets how frequently the lattice microstructure is refreshed to mimic ECM turnover: at times $t = k\,\tau_{ren}$ the bond configuration is regenerated with the same occupancy probability p. The observation time determines the duration over which we follow the cell trajectory. For convenience we nondimensionalise time by setting $\tau_{hop} = 1$, so that the random walker attempts one hop per unit time.

Let $P_i(t)$ denote the probability that the walker occupies lattice site i at time t. Its evolution is governed by a master equation

$$\dot{P}_i(t) = \sum_{j \neq i} P_j(t)\, w_{ji} - P_i(t) \sum_{k \neq i} w_{ik}, \qquad (1)$$

where w_{ji} is the probability per unit time to hop from site j to a neighbouring site i. On a regular lattice with coordination number n_c (for a square lattice $n_c = 4$) we normalise the rates so that $P_{i \neq j}\, w_{ji} = 1$ in our time units.

In the limit of very fast renewal, $\tau_{ren}/\tau_{hop} \ll 1$, the walker effectively perceives an averaged medium in which each bond is open with probability p, yielding $w_{ji} = p/n_c$. When the observation time encompasses many renewal events ($\tau_{obs}/\tau_{ren} \gg 1$) the motion becomes diffusive and the mean square displacement grows linearly in time, $\langle x^2 \rangle \propto t$, irrespective of the stationary-state distribution [27]. This dynamic–percolation framework allows us to explore how ECM turnover influences cellular migration.

For clarity a schematic representation of the lattice and movement rules is provided in Fig. 1: bonds (solid lines) denote occupied fibres ($E = 1$) and gaps (dashed) denote pores ($E = 0$). A cell located at a lattice site can only move along open bonds; this restricts its possible steps according to the instantaneous percolation configuration.

2.1. Radiotherapy-Induced ECM Dynamics

Experimental work suggests that radiation accelerates matrix turnover by activating fibroblasts and altering collagen crosslinking. To capture this effect we set the renewal probability pe proportional to the radiation dose. Specifically, we take

$$p_e = \frac{\tau_{\mathrm{hop}}}{\tau_{\mathrm{ren}}} = \gamma \times (\mathrm{Radiation\ dosage}),$$

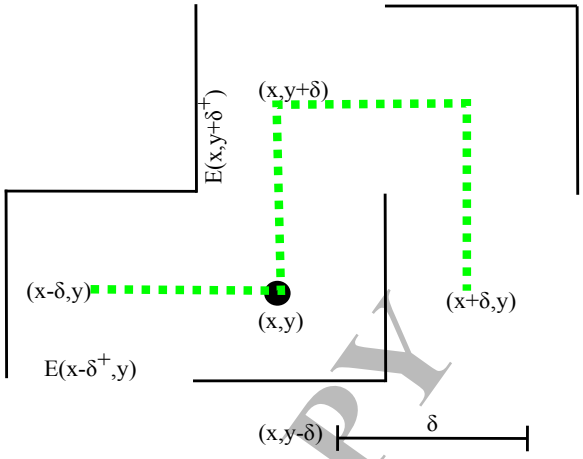

Figure 1: Schematic of the bond-percolation lattice used to represent the ECM. Bonds (solid lines) correspond to ECM fibres or steric obstacles ($E = 1$), whereas the absence of a bond represents an open pathway ($E = 0$). A cell located at lattice position (x,y) can move only along open bonds (for example along the dashed green path). Each bond is independently present with probability p and absent with probability $1 - p$, yielding a square bond–percolation model

where γ is a scaling constant. In our simulations $\gamma = 10^{-3}$ so that even modest doses increase the frequency of ECM remodelling. When no radiation is applied (dose zero) the lattice remains static; high doses drive rapid turnover and thus increase the effective diffusivity of the random walk.

2.2. Tumour Growth Model

To couple motility to population dynamics we introduce cell duplication. Each cell has a probability of division per unit time denoted p_{dup}. In our simulations we choose $p_{dup} = 0.01$ so that on average a cell divides once every hundred time units. The lattice is initially populated with cells clustered near the centre of the domain. Cells then perform random walks according to the rules above and may duplicate.

2.3. Tumour Growth under Radiotherapy

Radiotherapy is implemented as a probabilistic cell kill. At prescribed times a fraction of the living cells is removed. We set the kill probability for an individual cell to $p_{kill} = \eta \times$ (Radiation dosage), with $\eta = 10^{-3}$. This linear scaling ensures that higher dose treatments eliminate a larger fraction of cells. Combining duplication and killing allows us to examine how scheduling influences the net tumour burden.

2.4. Key Observables

Key observables in our study are the mean square displacement $\langle r^2(t)\rangle$ and the mean displacement $\langle r(t)\rangle$. On a log–log plot, these quantities exhibit power laws $\langle r^2\rangle \sim t^{2\alpha}$ and $\langle r\rangle \sim t\alpha$, where α characterises the nature of the motion: $\alpha < 0.5$ denotes sub-diffusion, $\alpha = 0.5$ normal diffusion and $\alpha > 0.5$ super-diffusion. We also measure the effective diffusion coefficient $D \equiv \langle r^2(t_{max})\rangle / (2dt_{max})$, where d is the spatial dimension and t_{max} is the observation time. For tumour dynamics we track the total number of cells as a function of time, allowing us to quantify how duplication and kill rates combine to determine overall growth or regression. *Result*:

2.5. Static ECM

To isolate the effect of matrix density, we first considered a static ECM in which the bond renewal probability was set to zero ($p_e = 0$). Figure 2 shows the mean square displacement (MSD) as a function of time for several bond-occupancy probabilities p. In the absence of renewal the walker is confined by static obstacles and the MSD grows sub-linearly in time. The displacement remains limited, reflecting the hindering effect of a fixed fibre network. An intermediate occupancy ($p \approx 0.5$) yields the largest MSD, but the motion remains sub-diffusive for all p.

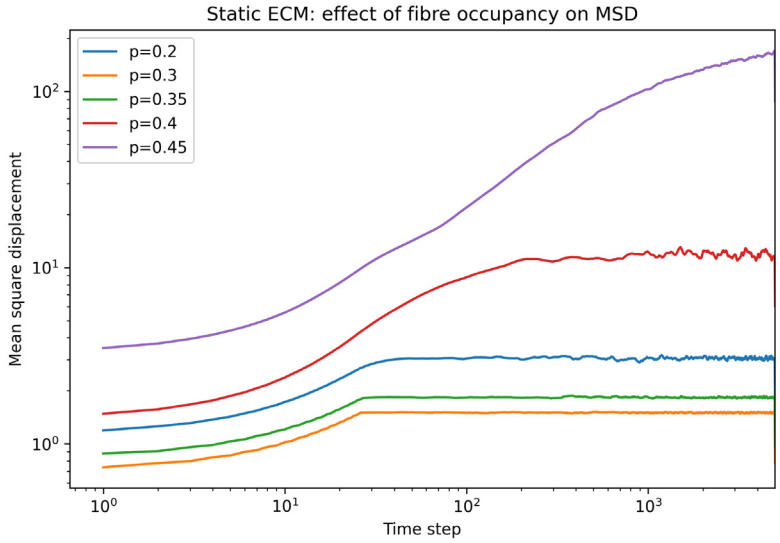

Figure 2: Mean square displacement (MSD) versus time for different bond-occupancy probabilities p in a static ECM. Each curve corresponds to a random percolation lattice with the indicated p and no bond renewal ($p_e = 0$). To assist visual estimation of the slope, dashed reference lines of unit slope and grid lines are included. The slope of the log–log curve at long times defines the transport exponent α

2.6. Dynamic ECM

We next investigated how bond renewal modifies cell motility. Figure 3 shows the MSD for a fixed bond occupancy p (here p = 0.4) and several renewal probabilities p_e. Even a small renewal probability dramatically enhances cell displacement: increasing p_e from 0 to 0.01 transforms the motion from sub-diffusive to nearly diffusive, and at $p_e \approx 0.1$ the MSD grows faster than linearly. This transition reflects the creation of transient pathways that bypass static obstacles. We quantified the transport exponent α and the normalised MSD at a fixed observation time t_{max} (not shown) and found that both increase monotonically with p_e, saturating at high renewal rates.

These results are consistent with experimental observations that dynamic reorganisation of the ECM promotes cell motility. In our model each bond is refreshed independently with probability p_e per time step and is set to be present with probability p, irrespective of the location of the walker. Varying p_e from 0 to 1 at a fixed occupancy p changes the MSD by orders of magnitude. For example, at p = 0.5 increasing the renewal probability from 0 to 0.1 transforms the motion from strongly sub-diffusive to nearly ballistic (Fig. 3).

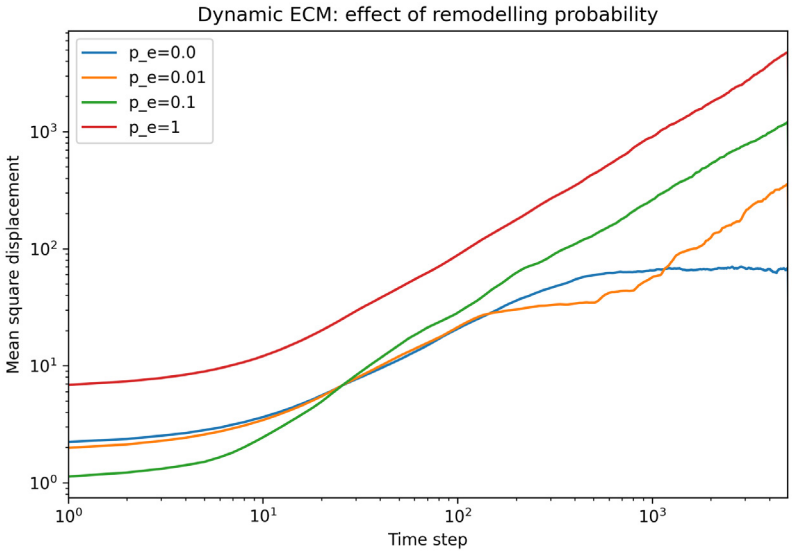

Figure 3: Mean square displacement (MSD) versus time for several bond renewal probabilities p_e at fixed occupancy p = 0.4. Increasing p_e accelerates migration and shifts the motion from sub-diffusive to diffusive or super-diffusive behaviour

2.7. Radiotherapy-Induced ECM Dynamics

Radiation does not simply kill tumour cells; it also stimulates stromal cells and modifies the biochemical and structural properties of the ECM. Experimental work suggests that irradiation accelerates matrix turnover by activating fibroblasts and altering collagen cross-linking. To capture this effect in a simple way we assume that the bond renewal probability p_e is proportional to the absorbed dose delivered per fraction. Specifically we set $p_e = \gamma D$, where D is the dose (in Gy) delivered in a given fraction and γ is a scaling constant. In our simulations we choose $\gamma = 10^{-3}$ so that modest doses produce small but noticeable increases in p_e. When no radiation is applied (D = 0) the lattice remains static; high doses drive rapid turnover and thus increase the effective diffusivity of the random walk (Fig. 4). This linear dependence is a first-order approximation valid for small doses. In reality the tissue response is likely to be nonlinear and may follow a sigmoidal dose–response curve, saturating at high doses when matrix damage and repair processes balance. Similarly, we model cell killing as a simple linear function of dose ($p_{kill} = \eta D$ with $\eta = 10^{-3}$). A more mechanistic description based on the linear–quadratic (LQ) model would set the instantaneous kill rate proportional to $(\alpha+2\beta D)RN$ (where R is the dose rate, N the number of tumour cells, and α and β tissue-specific radiosensitivity parameters) and would include sublethal damage repair during fractionation. These refinements are beyond the scope of the present work and are discussed as limitations in Sec. *V*.

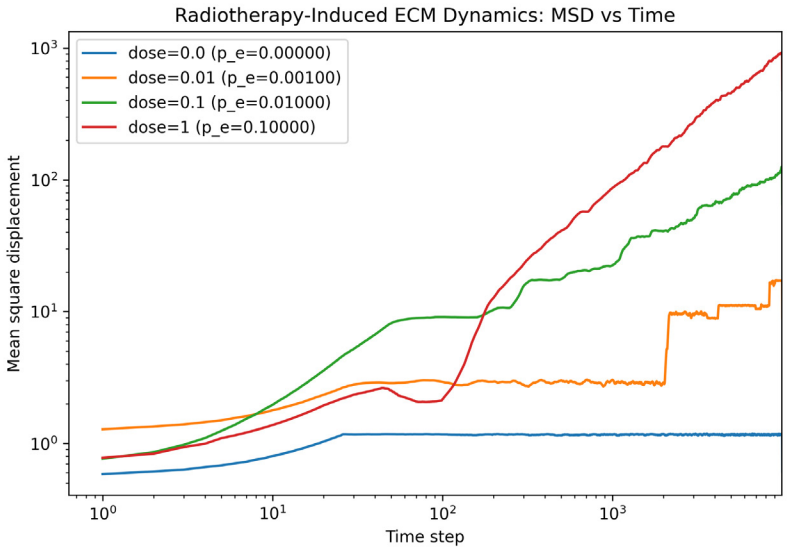

Figure 4: Mean square displacement (MSD) versus time for different values of radiotherapy dose and consequently pe at fixed bond occupancy p = 0.4. Radiation dose is reported in grays (Gy) and the renewal probability is given by pe = γD

2.8. Radiotherapy-Induced Growth Dynamics

Figure 5 shows the evolution of tumour cell populations under single-fraction radiotherapy at varying doses. While higher doses cause a more pronounced initial drop in cell number due to their stronger cytotoxic effect, they also lead to a faster relapse. This counterintuitive regrowth pattern arises from radiation-induced ECM remodelling: intense doses cause greater structural disruption of the matrix, which—once repaired—results in a more permissive microenvironment for tumour cell migration and proliferation. In contrast, moderate doses strike a balance between immediate cytotoxicity and long-term ECM preservation, delaying relapse.

To assess the effect of dose fractionation, we applied the same total radiation amount either as one, two, or four fractions spaced evenly in time (Fig. 6). Increasing the number of intermediate fractions consistently reduced final tumour size. This is because distributing the dose across multiple fractions maintains cumulative cytotoxicity while limiting the ECM damage per fraction, thereby slowing the migration-facilitated relapse.

Finally, we compared schedules in which the *same total dose* was administered either as a single prolonged pulse or as ten shorter pulses of equal magnitude delivered at regular intervals (Fig. 7). In the multi-pulse scenario the total absorbed dose is divided evenly across ten injections. The multi-pulse regimen consistently outperformed the single-pulse case in controlling long-term tumour size. Shorter, repeated pulses avoid prolonged ECM disruption, reduce the window for migration-driven spread between treatments, and sustain tumour suppression over time.

Taken together, these results suggest that careful optimisation of both dose magnitude and fractionation schedule can reduce tumour relapse risk by minimising ECM-mediated promotion of cell migration, without sacrificing cytotoxic efficacy.

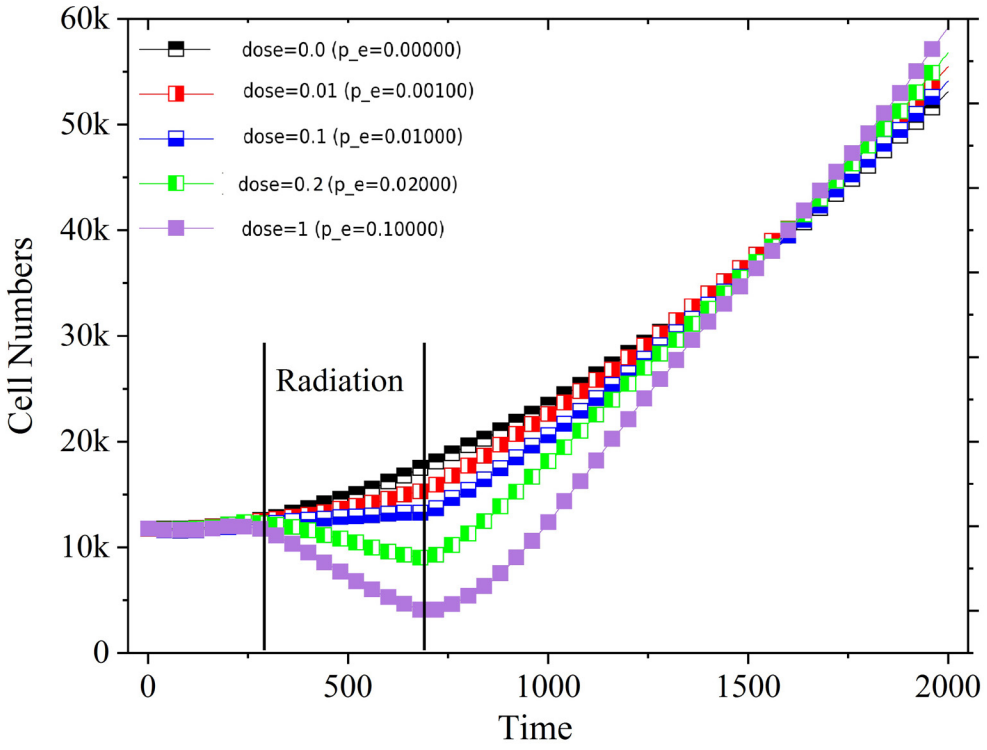

Figure 5: Number of cells versus time for different single-fraction doses (in Gy). Higher doses cause stronger initial tumour reduction but accelerate relapse through enhanced ECM remodelling. All simulations use the same scaling constant η for cell kill

3. Discussion

Our multi-scale modelling framework integrates cell motility on a dynamic percolation lattice with simple tumour growth and radiotherapy-induced cytotoxicity. This combination allowed us to probe how changes in extracellular matrix (ECM) turnover, either spontaneous or radiation-induced, influence both migration dynamics and tumour population outcomes.

In the absence of ECM remodelling ($p_e = 0$), cell displacement was severely limited, reflecting the role of a static ECM as a physical barrier to invasion. Introducing even modest remodelling rates transformed migration from subdiffusive to diffusive or super-diffusive regimes, in agreement with the idea that ECM turnover can open transient pathways through otherwise restrictive microenvironments. The relationship between p_e and motility was nonlinear, with rapid gains at low–intermediate p_e and saturation at high values. This suggests that there may be a threshold remodelling rate beyond which further ECM changes confer little additional advantage to migration.

When radiotherapy was included, the same parameter p_e became dose-dependent, representing accelerated ECM turnover due to treatment-induced fibroblast activation and collagen reorganisation. While higher doses produced an initial sharp decline in tumour cell numbers, they also led to faster relapse, likely because the accompanying ECM damage enhanced residual cell motility. This trade-off highlights the dual role of radiotherapy—cytotoxic to tumour cells, but also potentially pro-migratory through microenvironmental changes.

Treatment schedule simulations revealed that fractionation patterns influence tumour outcomes even when the total delivered dose is constant. Intermediate regimens, whether through multiple smaller doses or shorter inter-fraction intervals, were more effective at limiting long-term tumour growth compared to single high-dose treatments. This aligns with clinical observations that hypofractionation can sometimes be less beneficial for local control if it triggers rapid stromal remodelling.

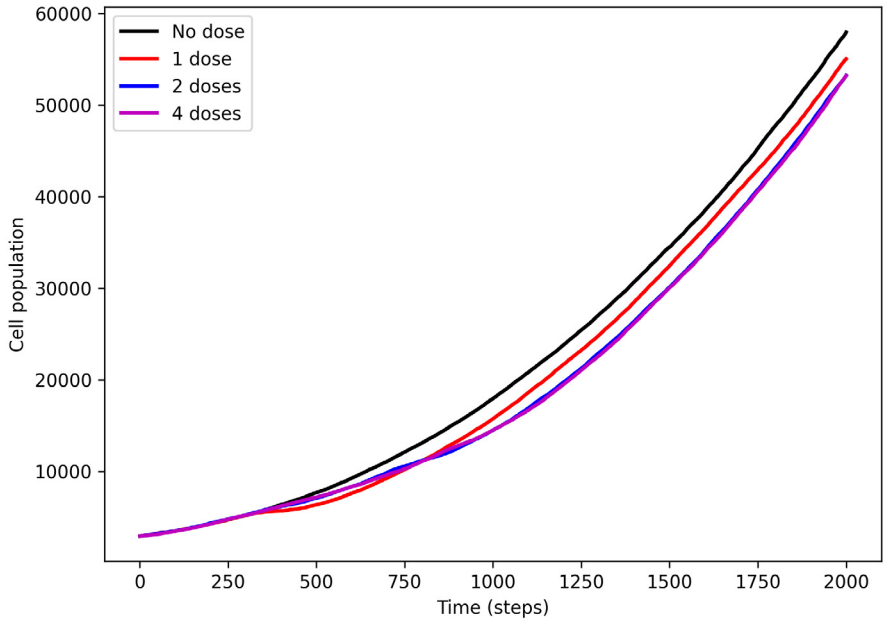

Figure 6: Number of cells versus time for equal total radiation delivered in one, two, or four evenly spaced doses. The total absorbed dose (Gy) is split into the indicated number of fractions delivered at regular intervals. More frequent intermediate doses lead to smaller final populations by mitigating ECM-driven regrowth

An additional observation from the static ECM simulations was the presence of an optimal ECM density ($p \approx 0.45$) for migration in dynamic conditions. This intermediate density appears to balance the availability of movement pathways with sufficient structure to facilitate effective displacement. Such a non-monotonic dependence has parallels in percolation theory and may have biological analogues in partially degraded or reorganised ECM during tumour progression.

Overall, our findings suggest that mathematical models coupling motility, microenvironmental change, and tumour growth can help explain why some radiotherapy regimens fail to prevent recurrence despite substantial initial tumour reduction. They also support the notion that preserving ECM integrity, or mitigating treatment-induced ECM remodelling, could be a therapeutic objective alongside direct tumour cell kill.

4. Conclusion

Our model provides a simplified yet insightful framework for studying how ECM structure and dynamics influence cell migration. By mapping cell motility to a random walker on a percolation lattice, we capture essential aspects of spatial heterogeneity and temporal remodelling in the tumour microenvironment.

The simulations confirm that static, randomly organised ECMs strongly restrict migration, supporting the view that structural alignment is important for long-range movement. However, dynamic remodelling—whether spontaneous or radiation-induced—renders even disordered ECMs permissive to migration. This may explain clinical observations of metastasis in tumours lacking aligned ECM: the inherent turnover of the matrix provides transient escape routes.

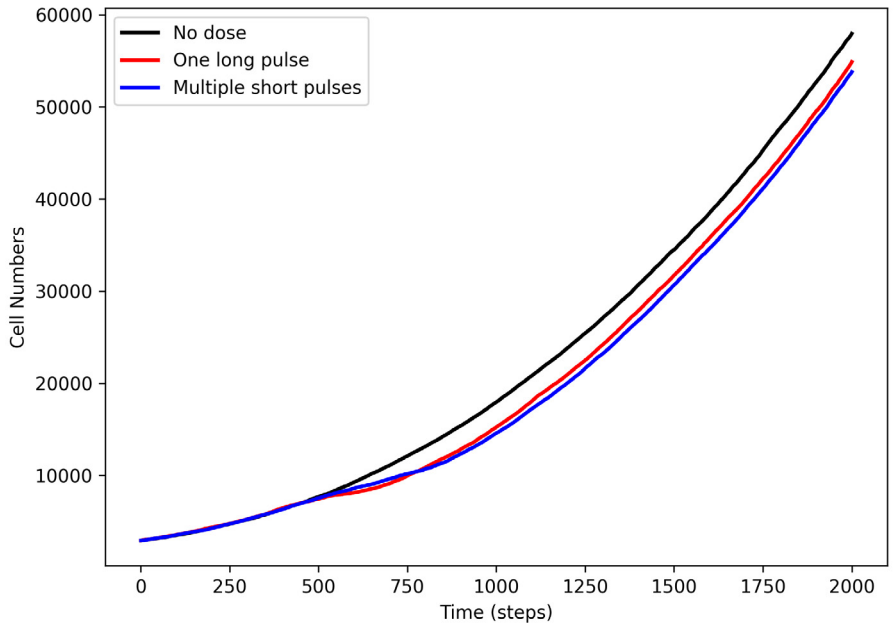

Figure 7: Number of cells versus time for equal total dose delivered either as one prolonged pulse or as ten shorter pulses separated by equal intervals. Each of the ten pulses delivers one-tenth of the total absorbed dose. Shorter pulses with shorter inter-fraction times achieve better long-term tumour control

Migration efficiency increases with ECM renewal rate (p_e) until saturation, highlighting a nonlinear relationship between matrix dynamics and cell dispersal. This has direct therapeutic implications: if radiotherapy accelerates ECM turnover, it could inadvertently promote metastatic spread despite its cytotoxic effects.

We also identify an optimal ECM density around $p \sim 0.45$ in dynamic conditions, where partial obstruction combined with high dynamism yields maximal migration. This mirrors experimental findings in which partial ECM degradation or reorganisation optimally supports invasive behaviour. In addition to providing mechanistic insight, our findings align with a growing body of evidence suggesting that moderate treatment regimens can achieve superior long-term control compared to maximum tolerated dose strategies. Mathematical oncology studies have demonstrated that intermediate dosing schedules may reduce selective pressure for resistant clones, preserve sensitive populations, and mitigate adverse microenvironmental remodeling, ultimately leading to improved therapeutic outcomes [28,29]. Such results underscore the potential of adaptive or intermediate fractionation approaches, where balancing cytotoxic effects with ecological and evolutionary tumor dynamics can be more effective than aggressive high-dose protocols [30]. By situating our framework within this broader modeling literature, we emphasize that radiotherapy optimization requires not only direct tumor cell killing but also careful consideration of the long-term ecological consequences of treatment intensity.

Our modelling framework is flexible and can be extended to account for anisotropic remodelling, chemotactic gradients, or collective cell effects, bringing it closer to physiological scenarios.

Limitations

While our model captures key interactions between ECM structure, tumour cell motility, and radiotherapy, it remains a simplified abstraction of the in vivo tumour microenvironment. First, ECM remodelling is represented as a uniform stochastic process across the lattice, whereas in reality, matrix turnover is spatially heterogeneous, cell-driven, and influenced by gradients of proteases, oxygen, and signalling molecules. Second, the tumour growth module is based on simple birth–death dynamics without incorporating nutrient diffusion, immune surveillance, angiogenesis, or mechanical feedback, all of which play significant roles in real tumours.

Radiotherapy effects were modelled using a linear dose–response for both cell kill and ECM remodelling rate, whereas in biological systems these relationships are often nonlinear, vary across cell types, and may depend on dose rate or fractionation history. Additionally, our model treats the cell population as homogeneous, not accounting for phenotypic heterogeneity or treatment-resistant subclones.

Finally, we did not explicitly include ECM anisotropy or directional guidance cues, which are known to influence migration and may interact with ECM turnover in non-trivial ways. Future work could incorporate anisotropic percolation lattices, chemotactic fields, and multi-cell interactions to capture collective invasion. Despite these limitations, the model highlights important trade-offs between cytotoxic effects and pro-migratory side effects of radiotherapy, providing a conceptual framework for exploring

treatment strategies.

Author Contribution

H.B. designed the study, wrote the codes and performed the analysis. H.B., J.K. and R.L. wrote and finalized the draft.

Data Availability

All codes and data are available upon request from the corresponding author.

Acknowledgment

Reference

1. Barcellos-Hoff, M. H., Park, C., & Wright, E. G. (2005). Radiation and the microenvironment–tumorigenesis and therapy. *Nature Reviews Cancer, 5*(11), 867-875.
2. Grigorieva, E. V. (2020). Radiation effects on brain extracellular matrix. *Frontiers in Oncology, 10*, 576701.
3. Schaue, D., & McBride, W. H. (2015). Opportunities and challenges of radiotherapy for treating cancer. *Nature reviews Clinical oncology, 12*(9), 527-540.
4. Lu, P., Takai, K., Weaver, V. M., & Werb, Z. (2011). Extracellular matrix degradation and remodeling in development and disease. *Cold Spring Harbor perspectives in biology, 3*(12), a005058.
5. Gattazzo, F., Urciuolo, A., & Bonaldo, P. (2014). Extracellular matrix: a dynamic microenvironment for stem cell niche. *Biochimica et Biophysica Acta (BBA)-General Subjects, 1840*(8), 2506-2519.
6. Keating, M., Kurup, A., Alvarez-Elizondo, M., Levine, A. J., & Botvinick, E. (2017). Spatial distributions of pericellular stiffness in natural extracellular matrices are dependent on cell-mediated proteolysis and contractility. *Acta biomaterialia, 57*, 304-312.
7. Bauer, A. L., Jackson, T. L., & Jiang, Y. (2009). Topography of extracellular matrix mediates vascular morphogenesis and migration speeds in angiogenesis. *PLoS computational biology, 5*(7), e1000445.
8. Smith, M. L., Gourdon, D., Little, W. C., Kubow, K. E., Eguiluz, R. A., Luna-Morris, S., & Vogel, V. (2007). Force-induced unfolding of fibronectin in the extracellular matrix of living cells. *PLoS biology, 5*(10), e268.
9. Wood, A. (1988). Contact guidance on microfabricated substrata: the response of teleost fin mesenchyme cells to repeating topographical patterns. *Journal of cell science, 90*(4), 667-681.
10. Webb, A., Clark, P., Skepper, J., Compston, A., & Wood, A. (1995). Guidance of oligodendrocytes and their progenitors by substratum topography. *Journal of cell science, 108*(8), 2747-2760.
11. Gomez, N., Chen, S., & Schmidt, C. E. (2007). Polarization of hippocampal neurons with competitive surface stimuli: contact guidance cues are preferred over chemical ligands. *Journal of The Royal Society Interface, 4*(13), 223-233.
12. Teixeira, A. I., Abrams, G. A., Bertics, P. J., Murphy, C. J., & Nealey, P. F. (2003). Epithelial contact guidance on well-defined micro-and nanostructured substrates. *Journal of cell science, 116*(10), 1881-1892.
13. Loesberg, W. A., Te Riet, J., Van Delft, F. C. M. J. M., Schön, P., Figdor, C. G., Speller, S., ... & Jansen, J. A. (2007). The threshold at which substrate nanogroove dimensions may influence fibroblast alignment and adhesion. *Biomaterials, 28*(27), 3944-3951.
14. Nakatsuji, N., & Johnson, K. E. (1982). Cytoskeleton 2, 149.
15. Nakatsuji, N., & Johnson, K. E. (1984). Ectodermal fragments from normal frog gastrulae condition substrata to support normal and hybrid mesodermal cell migration in vitro. *Journal of cell science, 68*(1), 49-67.
16. Nakatsuji, N., & Johnson, K. E. (1984). Experimental manipulation of a contact guidance system in amphibian gastrulation by mechanical tension. *Nature, 307*(5950), 453-455.
17. Sidani, M., Wyckoff, J., Xue, C., Segall, J. E., & Condeelis, J. (2006). Probing the microenvironment of mammary tumors using multiphoton microscopy. *Journal of mammary gland biology and neoplasia, 11*(2), 151-163.
18. Provenzano, P. P., Inman, D. R., Eliceiri, K. W., Knittel, J. G., Yan, L., Rueden, C. T., ... & Keely, P. J. (2008). Collagen density promotes mammary tumor initiation and progression. *BMC medicine, 6*(1), 11.
19. Provenzano, P. P., Inman, D. R., Eliceiri, K. W., Trier, S. M., & Keely, P. J. (2008). Contact guidance mediated three-dimensional cell migration is regulated by Rho/ROCK-dependent matrix reorganization. *Biophysical journal, 95*(11), 5374-5384.
20. Anderson, A. R., Weaver, A. M., Cummings, P. T., & Quaranta, V. (2006). Tumor morphology and phenotypic evolution driven by selective pressure from the microenvironment. *Cell, 127*(5), 905-915.
21. Lowengrub, J. S., Frieboes, H. B., Jin, F., Chuang, Y. L., Li, X., Macklin, P., ... & Cristini, V. (2010). Nonlinear modelling of cancer: bridging the gap between cells and tumours. *Nonlinearity, 23*(1), R1-R91.
22. Byrne, H. M. (2010). Dissecting cancer through mathematics: from the cell to the animal model. *Nature Reviews Cancer, 10*(3), 221-230.
23. Rockne, R. C., Hawkins-Daarud, A., Swanson, K. R., Sluka, J. P., Glazier, J. A., Macklin, P., ... & Scott, J. G. (2019). The 2019 mathematical oncology roadmap. *Physical biology, 16*(4), 041005.
24. Jeong, J., Shoghi, K. I., & Deasy, J. O. (2013). Modelling the interplay between hypoxia and proliferation in radiotherapy tumour response. *Physics in medicine and biology, 58*(14), 4897-4919.
25. Anderson, A. R. (2005). A hybrid mathematical model of solid tumour invasion: the importance of cell adhesion. *Mathematical medicine and biology: a journal of the IMA, 22*(2), 163-186.
26. Azimzade, Y., Saberi, A. A., & Sahimi, M. (2019). Effect of heterogeneity and spatial correlations on the structure of a tumor invasion front in cellular environments. *Physical Review E, 100*(6), 062409.

27. Druger, S. D., Nitzan, A., & Ratner, M. A. (1983). Dynamic bond percolation theory: A microscopic model for diffusion in dynamically disordered systems. I. Definition and one-dimensional case. *The Journal of chemical physics, 79*(6), 3133-3142.
28. Gatenby, R. A., Silva, A. S., Gillies, R. J., & Frieden, B. R. (2009). Adaptive therapy. *Cancer research, 69*(11), 4894-4903.
29. Staňková, K., Brown, J. S., Dalton, W. S., & Gatenby, R. A. (2019). Optimizing cancer treatment using game theory: a review. *JAMA oncology, 5*(1).
30. Yin, A., van Hasselt, J. G., Guchelaar, H. J., Friberg, L. E., & Moes, D. J. A. (2022). Anti-cancer treatment schedule optimization based on tumor dynamics modelling incorporating evolving resistance. *Scientific reports, 12*(1), 4206.